ABSORPTION CHARACTERISTICS OF MULTI-LAYERED SPHERE MODELS EXPOSED TO UHF/MICROWAVE RADIATION

Claude M. Weil
Environmental Protection Agency
Research Triangle Park, N. C. 27711

Abstract

Plane wave absorption characteristics of spherical models composed of six layers of dissipative dielectric media, representing various biological tissues found in human and animal heads, are examined in the frequency range of 0.1 to 10 GHz. The internal distribution of energy deposition inside the sphere is discussed with emphasis on strong localized heating (hot spot) effects.

Introduction

In any studies involving the biological effects of microwave radiation on humans or animals, the absorbed radiation dosage is of paramount importance. The dosimetry problem has two basic aspects: a) the efficiency of total energy coupling into the subject undergoing exposure (i.e., the absorption cross section) and b) the internal distribution of R. F. energy within that subject. Both of these depend in turn on the following factors: the wavelength of the incident waves and the size, shape and composition of the irradiated subject, as well as its outside curvature. In general, coupling is most efficient when the modified wavelength (i.e., that within the biological media) approximates the dimensions of the subject: however, the internal energy distribution for this case is rarely a uniform one and significant localized heating (hot spots) can be created. When the wavelength is much shorter than the subject size, penetration is poor and most of the incident energy is deposited on the body surface (this is the only case where the so-called slab model for tissues is valid).

It is, in general, virtually impossible to solve the dosimetry problem for the case of a very complex biological subject, such as a human or a laboratory animal, exposed to an often equally complex radiation source, such as that present in the near field of a horn antenna. For this reason, previous workers have utilized simpler models, such as a sphere of dissipative and homogeneous media, having much the same dielectric characteristics as some biological material such as muscle or brain, exposed to the simplest form of radiation (i.e., a plane wave). Such a model is a crude representation of animal and human heads and the problem is readily solvable by means of high-speed machine computations. Results from this simplified model can provide useful guidelines to workers frequently confronted with more complex dosimetry problems.

Formulation of Problem

Figure 1 shows the six-layered model used in this study, with a plane wave, polarized in the x-direction and propagating in the z-direction, incident upon it. The outer most region (p = 7) or sixth layer represents air. The dielectric properties and layer thicknesses of the remaining regions (p = 1,2,3,4,5, 6), consisting of a core of brain-like matter and five concentric layers, are summarized in Table 1 for three different sized spheres (6.6, 12 and 20 cms diameter).

Tissue electrical properties were obtained from values measured and published by Schwan [1], Presman [2] and others. Variations of ±30% or more can exist in the figures quoted. The changes of electrical characteristics with frequency are significant and were incorporated into all aspects of this work; sets of average curves giving permittivity and conductivity changes with frequency for the various tissues modeled, were prepared and stored in a data bank.

Expansion of the incident and secondary (scattered and internally induced) fields into vector spherical harmonics is based on Stratton's formulation [3]. Tangential components of E and H-fields are then equated at the six regional boundaries in order to determine the unknown expansion coefficients. Further, details are given in Shapiro's work [4] (see also Figure 1).

Absorption Properties

The overall scattering and absorption properties of an object exposed to electromagnetic waves are usually defined in terms of scattering and absorption cross sections (the cross sectional areas of a flat perfect reflector or absorber, placed normal to the incident waves, which will scatter or absorb energy in the same amount as the original object). The relative absorption cross section (RACS) of an object may be defined as its absorption cross section, Q_A divided by its geometric or shadow cross section (πr^2 for the case of a sphere). In Figure 2, the RACS is plotted against frequency for both our six layer model and a homogeneous sphere (no extra layers) of similar size (6 cms radius). Note the significant difference between the two cases. If a series of such curves is obtained for various multi-layered models, ranging in size from 2 to 12.5 cms radii, we can develop a contour plot of radius versus frequency which readily

TABLE 1

Region (P)	Tissue Modeled	Electrical Properties of Tissue at 10^9 Hz		Core Size and Layer Thickness, cms		
		Relative Permittivity	Conductivity (ohm-m)$^{-1}$	Outer Radius r_6 = 3.3cms	6cms	10cms
1	Brain	60	0.9	r_1=2.68	r_1=5.27	r_1=9.10
2	CSF	76	1.7	0.2	0.2	0.2
3	Dura	45	1.0	0.05	0.05	0.50
4	Bone	8.5	0.11	0.2	0.28	0.4
5	Fat	5.5	0.08	0.07	0.1	0.15
6	Skin	45	1.0	0.1	0.1	0.1

shows where the absorption is greatest and where it is weak. Examination of Figure 3 indicates that two main "ridge" lines (shown dotted) are apparent; these indicate that optium energy coupling exists for such combinations of sphere size and frequency. Note also that the absorption cross section can exceed the shadow cross section by 40% or more at certain frequencies.

Dose Distribution

The second aspect of the dosimetry problem involves the internal distribution of induced fields inside the model. Kritikos and Schwan [5] and Johnson and Guy [6] have determined internal distributions for various sphere size-frequency combinations using the simple homogeneous model. Shapiro, et al. [4] repeated this, using the six layer model, but only for one specific size and frequency. All of these workers discovered significant localized heating (or hot spots) hear the sphere center, caused by standing wave effects and energy focusing. However, they only examined field distributions along the x, y or z axes. Figures 4 and 5 show sections through the core of our 6 layer model (radius 6 cms) taken in the $\phi = 0$ plane. This corresponds to the E plane of the incident wave. The contours represent lines of equal normalized heating potential, $1/2\ \sigma_1 \left|\frac{E}{E}\right|^2$ where σ_1 is the conductivity of the core material (brain). The frequency of 790 MHz utilized in Figure 4 was selected using the first (left) "ridge" line of Figure 3 for a 6 cms radius sphere, where coupling is optimum. It is evident from Figure 4 that radiation at this frequency does indeed create a hot spot on the z-axis, just in front of the sphere center. However, increasing the frequency to 1250 MHz now creates two off-axis energy peaks located behind the center that are more intense and concentrated in a smaller volume. Still higher peaks, that gradually travel along the 1 cm circle toward the $\theta = 0$ radial as frequency is increased, will result; a maximum is reached at about 1650 MHz. This is illustrated in Figure 6, which shows plots of peak and average heating potentials versus frequency for an incident field of 10 mW/cm^2. Data for peak surface heating is also included and it can be seen that surface heating greatly exceeds peak internal heating for frequencies above 2250 MHz. Similar data were developed for the 3.3 and 10 cms radii spheres.

Conclusions

Significant differences are apparent between the homogeneous sphere and the six-layered model studied here. The latter absorbs more incident energy above 1000 MHz and the internal energy concentrations are far more significant in the smaller size spheres (up to 6 cms radius) than in the larger spheres where path lengths are greater and fields are more attenuated. This is of obvious significance to those involved in animal experimentation with microwave, since a given incident field level creates a much greater thermal burden for a small animal such as a rat or a mouse than it will for larger size species such as a dog or a human; also the dose distribution is much more locally concentrated for rats than it is for man. Great care is therefore needed in interpreting results obtained with animals.

Acknowledgments

We wish to thank the RAND Corporation, Santa Monica, California for the use of computer programs used in this study.

References

1. H.P. Schwan. "Radiation Biology Medical Applica- Radiation Hazards: in Microwave Power Engineering, Vol. 2, ed. by E.C. Okress, Academic Press, N.Y., 1968, pp. 215-234.

2. A.S. Presman. Electromagnetic Fields, Life. Plenum Press, N.Y., 1970, pp. 33-44.

3. J. Stratton. Electromagnetic Theory. McGraw-Hill, N.Y., 1941, p.565.

4. A.R. Shapiro, R.F. Lutomirski, H.T. Yura. "Induced Heating Within a Cranial Structure Irradiated by an Electromagnetic Plane Wave," IEEE Trans. Microwave Theory & Techs., MTT-19, pp. 187-196 (Feb. 1971).

5. H.N. Kritikos and H.P. Schwan. "Hot Spots Generated in Conducting Spheres by Electromagnetic Waves; Biological Implications," IEEE Trans. Biomed. Engin., BME-19, pp. 53-58, (Jan. 1972).

6. C.C. Johnson and A.W. Guy. "Nonionizing Electromagnetic Wave Effects in Biological Materials and Systems," Proc. IEEE, Vol. 60, pp. 692-718 (June 1972).

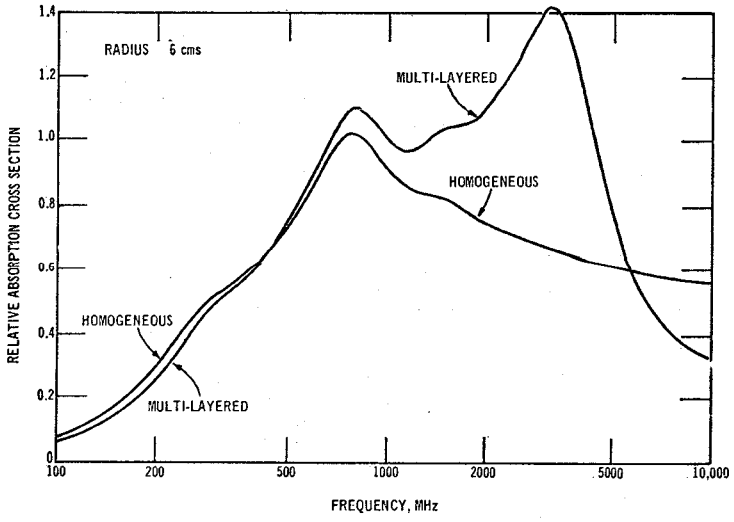

FIG. 2 Relative absorption cross section (RACS) versus frequency for homogeneous and six-layered spheres.

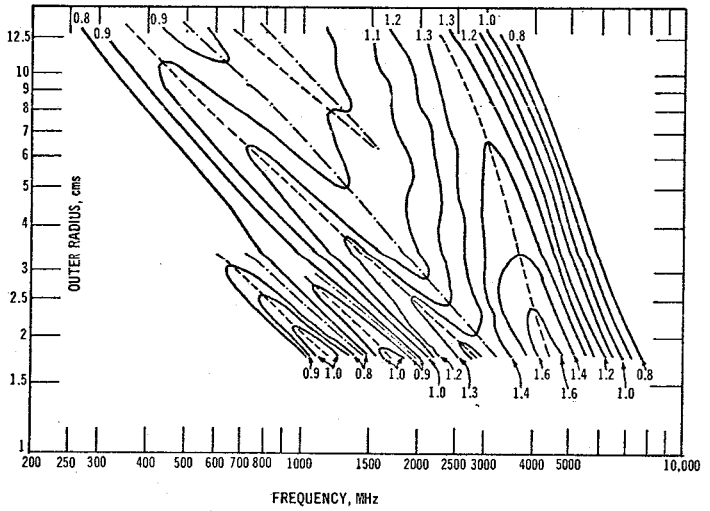

FIG 3 Radius v. frequency diagram for six-layered sphere; the contours represent lines of constant RACS.

Spherical Harmonic Expansions for Electric Fields

Incident:

$$\mathbf{E}_i = E_0 e^{-i\omega t} \sum_{n=1}^{\infty} i^n \frac{2n+1}{n(n+1)} \left(\mathbf{m}_{o1n}^{(1)} - i\mathbf{n}_{e1n}^{(1)}\right),$$

Reflected:

$$\mathbf{E}_r = E_0 e^{-i\omega t} \sum_{n=1}^{\infty} i^n \frac{2n+1}{n(n+1)} \left(a_n^r \mathbf{m}_{o1n}^{(3)} - ib_n^r \mathbf{n}_{e1n}^{(3)}\right),$$

Induced within sphere:

$$\mathbf{E}_t = E_0 e^{-i\omega t} \sum_{n=1}^{\infty} i^n \frac{2n+1}{n(n+1)} \left(a_n^t \mathbf{m}_{o1n}^{(1)} - ib_n^t \mathbf{n}_{e1n}^{(1)}\right),$$

Scattering Cross Section:

$$Q_s = \frac{2\pi}{k_2^2} \sum_{n=1}^{\infty} (2n+1)\left(|a_n^r|^2 + |b_n^r|^2\right)$$

Total Cross Section:

$$Q_t = \frac{2\pi}{k_2^2} Re \sum_{n=1}^{\infty} (2n+1)\left(a_n^r + b_n^r\right)$$

Absorption Cross Section, $Q_a = Q_t - Q_s$

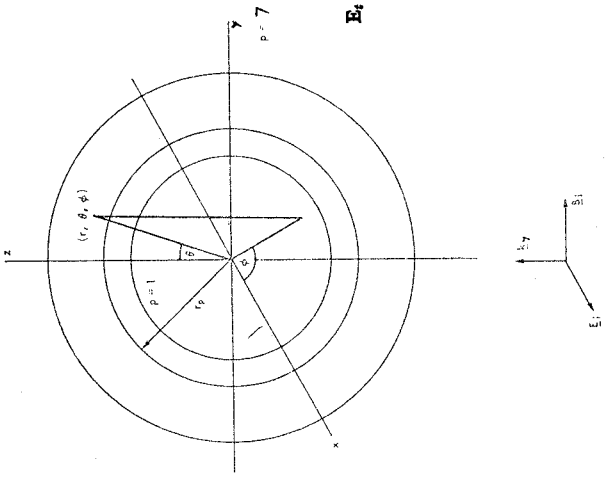

FIG. 1 Plane wave incident upon spherical model with six concentric shells.

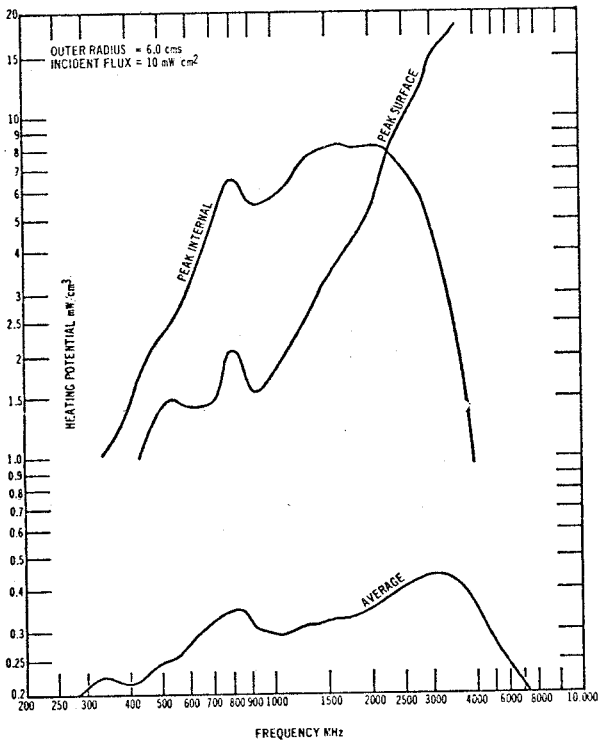

FIG. 6 Average and peak heating potentials versus frequency for 6 cms radius model (10mW/cm^2 incident)

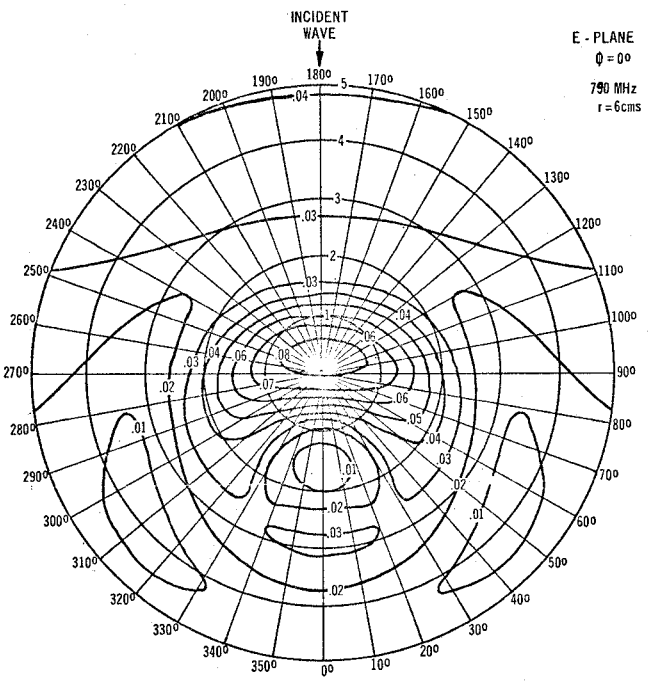

FIG. 4 Distribution of normalized heating potential in E-plane of sphere at 790 MHz.

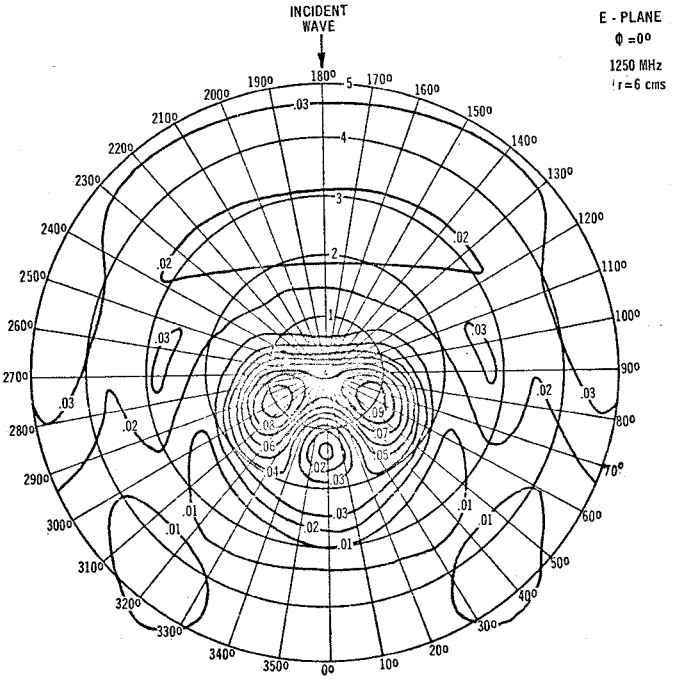

FIG. 5 Similar distribution for same sized sphere at 1250 MHz.